[1]Suvaditya Majumdar

[2]Shuvam Saha

[3]Dipayan Das

[4]Sudipta Chattopadhyay

Cooperative Spectrum Sensing based Novel Network Communication Schemes for Urban, Rural and Sub-Urban Areas

Journal of Electrical Systems

Abstract: - Cognitive Radio (CR) is an efficient spectrum sensing technique, which allows the secondary or unlicensed users to access the radio spectrum dynamically and opportunistically without interfering with the services of primary or licensed users. Cooperative Spectrum Sensing (CSS) is a CR spectrum sensing technique, where several nodes act in cooperation to detect the presence or absence of Primary User (PU). In this paper, both centralized and distributed aspects of CSS have been explored to Rural, Sub-Urban and Urban regions, operating under various atmospheric fading conditions. The entire work has been divided into three parts. In the first part, a new voting rule has been incorporated in Centralized CSS for Metropolitan Area Network (MAN) and its performance has been studied in terms of Region of Convergence (ROC) curves and Total Error (T.E.) under different fading conditions. In the second part, Distributed Cooperative Spectrum Sensing (DCSS) approach has been used to develop a Regional Area Network (RAN) for rural region incorporating various voting rules and fading conditions. Subsequently, the performance of this model has been studied considering an important metric, Detection Probability (DP). In the final part, a new region called sub-urban has been introduced in between the urban and rural and a combined model has been proposed and tested for all these regions considering various atmospheric attenuation factors like rain and fog. Finally, the performances of all these models have been compared with some of the existing related works.

Keywords: Cognitive Radio Networks, Cooperative Spectrum Sensing, Centralized Spectrum Sensing, Distributed Spectrum Sensing, Voting Rule

I. INTRODUCTION

Due to rapid growth of wireless devices, there has been a serious problem of short- age of frequency bands in the radio spectrum. Cognitive Radio technique proposes to solve this conflict between spectrum scarcity and spectrum under-utilization [1]. The radio spectrum can be efficiently utilized with the help of CR technique which uses both the Primary Users (PU) and Secondary Users (SU) in the network. Spectrum sensing techniques are used to sense the frequency bands of radio spectrum. Various helpful detection schemes to identify the spectrum holes in the given radio spectrum have been described in [1–3]. Numerous detection techniques have been developed to determine the activity of a licensed user. The simplest signal detection technique to identify the activity of a PU is the Energy Detection (ED) approach, where the prior knowledge of the PU signal is not needed [4]. In cases, where the SU experiences shad- owing or multipath fading, a new challenge called hidden terminal problem emerges [3]. In such scenarios, the Signal-to-Noise Ratio (SNR) of the received signal is typically low, rendering the SU incapable of reliably detecting the presence of the PU. Consequently, the SU erroneously perceives the frequency band as unoccupied and proceeds to utilize it, unaware of the PU's existence. To mitigate this issue, multiple SUs collaborates to perform spectrum sensing cooperatively.

Cooperative Spectrum Sensing (CSS) is particularly advantageous in different fading channels, as it enhances the likelihood of detecting the PU's presence, even in challenging fading conditions [5]. To facilitate the analysis of cooperative sensing, CSS is classified into two categories based on how cooperating CR users share the sensing data in the network, Centralized and Distributed. In Centralized Cooperative Spectrum Sensing (CCSS), local sensing results are reported at a common receiver, known as the Fusion Center (FC), that is in charge of making a global decision [6]. On the other hand, in Distributed Cooperative Spectrum Sensing (DCSS), the SUs exchange their sensing results among themselves without need of any additional infrastructure [6], [7]. One of the basic applications of CSS was presented in [8], where the spectrum sensing capabilities of CR networks were enhanced by employing an ED approach within the radio environment. To handle individual sensing challenges effectively, CCSS was introduced. Decision fusion rules, such as AND, OR, and MAJORITY, were applied under various scenarios for enhancing the performance of CCSS to the further extent. Among the three fusion rules, the MAJORITY fusion rule demonstrated superior performance for lower thresholds and reduced Total Error Rates

[1] *Corresponding author: ETCE Department, Jadavpur University, Kolkata, 700032, India; Institute of Engineering and Management Kolkata, University of Engineering and Management Kolkata

[2] ETCE Department, Jadavpur University, Kolkata, 700032, India

[3] ETCE Department, Jadavpur University, Kolkata, 700032, India

[4] ETCE Department, Jadavpur University, Kolkata, 700032, India

(TER) in similar scenarios. For better performance at higher thresholds, the performance of CSS was examined based on filtered energy detector with various fusion rules [9].

Additionally, the performance of CSS was discussed in [10] and [11] with diversity reception. To mitigate this effect of diversity, hard and soft fusion techniques for CSS were explored in [12] under noisy environment. In this work, the authors provided analytical equations for hard and soft one-bit and two-bit CSS combination methods, which was further improvised in [13]. This work proposed a double-threshold ED based CSS and delved into a hybrid censorship system based on both hard and soft fusion. In this context, [14–16] improvised the traditional ED based spectrum sensing approaches and used some factors like computational complexity, accuracy, and estimation speed to analyze the network utility functions and error probabilities. This was used to optimize MAJORITY voting rule approach of "N out of K" rule and determine the optimal number of CRs. In the realm of CR technology, spectrum sensing plays a critical role in identifying available spectrum resources for SUs. In [17], an optimal voting rule was employed for CSS while minimizing TER. The overall performance was assessed in the presence of additive white Gaussian noise (AWGN) as well as Rayleigh fading channels. This study proposed a low-energy spectrum sensing algorithm that required fewer cognitive users to achieve a specified error bound, thereby optimizing the utilization of CR resources. The performance of CCSS in different fading environments was further experimented in [18], where an ED based CSS scheme for Rayleigh fading channels was proposed. This approach leveraged multiple antennas at each CR to enhance spectrum sensing in challenging fading conditions. Furthermore, Nallagonda et al. investigated an improved ED based CR system with multiple antennas, considering both Rician and Hoyt fading channels [19]. It is important to note that the study in [19] did not examine the detection performance based on ideal parameters. In [20], researchers explored enhanced ED based CSS in the presence of both AWGN and Rayleigh fading channels. Moving over to a more urban scenario, Verma et al. presented an ED based CR sensing approach over Nakagami fading channels, incorporating Maximum Ratio Combining (MRC) diversity reception [21]. However, it is worth noting that the work in [21] was focused on a single CR user within a non-cooperative setting. To incorporate it in CSS, a novel CSS model with diversity was proposed [22] to improve detection accuracy and mitigate the effects of shadowing and fading characteristics using the OR-rule. The study highlighted the significant impact of fading channels on the detection capabilities of ED.

In contrast to CCSS, Distributed approaches have been emerged as the better option, where any one of the participating SUs can take the final decision before forwarding it to the next tier. In a typical DCSS, two stage decision is required, where the intra- cluster and inter-cluster sensing can use either same or a combination of two different voting rules [23]. A comparison between DCSS and CCSS was provided, considering various fading channels as mentioned in [6] earlier. It has been found that CSS in the presence of Nakagami fading is exposed to relatively limited attention. Additionally, the study acknowledged the challenges posed by mobile CR users in some applications, where channel estimation could be prohibitively costly. Despite these challenges, DCSS over Nakagami fading was found to be effective for system design, offering adaptability across a wide range of SNR and diverse decision fusion scenarios. The performance of DCSS was further investigated in Weibull and Hoyt fading channels [7] as cited before. It was observed that under various fusion rules such as AND-AND, AND-OR, OR-AND, and centralized AND, the performance of the Weibull fading channel outperforms the Hoyt fading channel. In [24], Halima et al. proposed a novel CSS scheme using Distributed Relay Selection. This algorithm activates relays when the SNR of the PU signal exceeds a predetermined threshold. However, when more than two relays have SNRs above the threshold, collisions occur, limiting PU signal detection. The study also explored Partial Relay Selection and Opportunistic Amplify Sensing, distinguishing them from centralized relay selection. Specifically, the relays with the highest SNR get activated, ensuring improved spectrum sensing. To enhance sensing performance and reduce reporting inaccuracies, a distributed architecture for processing and fusing sensing data was presented in [25]. In congested network conditions, decision fusion for cooperative users can be challenging, and reporting sensing traffic may consume excessive bandwidth. Here, a novel cooperative distributed PU detection approach has been proposed incorporating a dynamic threshold based on controlled probabilities of false alarms to enhance sensing efficiency and reliability in a Rayleigh fading environment. Fusion Nodes (FNs) were dynamically selected from group members, enabling cooperative distributed PUs detection. The adaptive detection threshold was calculated dynamically using Link Quality Indicators (LQIs) of sensing channels. Additionally, this approach significantly reduced the volume of data typically transmitted through reporting channels. Simulation results demonstrated that the revised threshold significantly improved the performance of the distributed cooperative sensing (DCS) process, reducing errors in terms of Probability of Detection (P_d) and Probability of False Alarm (P_f).

Above review shows that the concept of fading environment plays a very crucial role for both DCSS and CCSS. Apart from the existing fading models, incorporation of the atmospheric fading conditions such as rain and fog in a CR model makes it more realistic and robust. Though atmospheric fading is more dominant for a Regional Area Network (RAN) with larger distance and for microwave communications [26], the effect of rain and fog

attenuations for Metropolitan Area Networks (MAN) and Wide Area Networks (WAN)cannot be ignored. Few other geographical factors such as the presence of wet foliage, rain pattern, rain drop size and pattern, wind direction, etc. also plays a predominant role in Rural and Sub-Urban scenarios [27]. In context to the environmental fading, the rain specific attenuation for tropical regions for millimetre waves was presented in [28, 29]. Another ITU-R based rain predictive model was presented in [30]. Several other predictive Rain models were described in [31–37] and smart predictive models for fog attenuation was presented in [38].

Based on the analysis of the above research, this work makes an attempt to enhance the performance of the existing CCSS and DCSS architectures by proposing new voting rules. Here, CCSS model has been assigned for Urban Home Area Networks (HAN) and Field Area Networks (FAN); whereas, DCSS has been mapped to Rural and Sub-Urban networks. Moreover, a hybrid model has been developed combining both Urban CCSS model and Rural DCSS model. A third zone, namely Sub-Urban has been introduced in between Urban and Rural zones. In context to the atmospheric attenuations, the basic ITU-R model has been modified to generate a new distance and frequency-based rain attenuation model which can be scaled to our working frequency range of 2.5 to 3.5 GHz. In line with this, a novel Fog attenuation model for CSS has also been presented. These atmospheric attenuation models have been incorporated along with other fading models for a real life Urban, Rural, and Sub-Urban scenario.

The major contributions of this paper have been listed below:

- A Centralized CSS model for MAN has been developed for Urban region incorporating a new voting rule and tested for various fading conditions.
- A Distributed scheme of CSS for RAN has been proposed to cater the Rural region and the performance of the model has been evaluated with respect to different distributed voting rules and Rural fading environments.
- A Combined Model has been developed incorporating both centralized model and hybrid distributed model of CSS for Sub-Urban regions.
- Performance of the proposed Combined Model has been evaluated considering different rain and fog attenuation models.
- Performances of all the proposed models have been compared with related contrast models.
- Finally, superiority of all the proposed models has been established through performance analysis.

II. System Model

A general CSS model is described in Figure 1 comprising of one PU with dedicated sensing channels for the incumbent users. The Secondary CRs, that is, SUs opportunistically communicate through these sensing channels with the PU. The SUs have dedicated reporting channels with the FC. The SUs forward the sensed data to the FC which communicates the final decision to the PU via SUs.

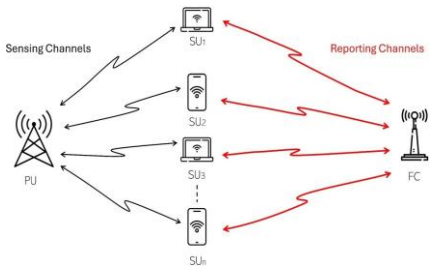

Figure 1: Generalised CSS Model

The system model for this proposed work has been described in three parts: Firstly, the CCSS approach to cater primarily the Urban segment; secondly, the DCSS approach to mainly incorporate the Rural area; finally, the Combined Centralised and Distributed approach targeted for Urban, Sub-Urban and Rural areas. All three parts are discussed in the following sub-sections. It is to mention that neither of these proposed models has considered the mobility and hand-off issues while discussing.

1.1 System model for CCSS

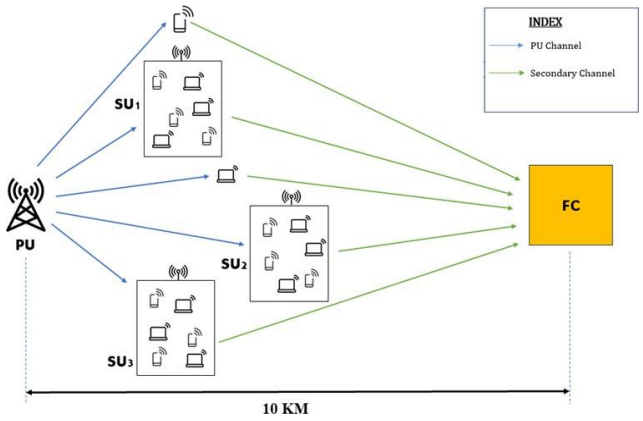

FIGURE 2 Proposed system model for Centralized CSS in Metropolitan Area Communication

In this proposed model as depicted in Figure 2, we have used the CCSS approach. The IEEE 802.16 standard [39] has been chosen for the MAN [39] having a communication range of 10km, frequency ranging from 2.5 GHz to 3.5 GHz with a data range from 11 Mbps to 7000 Mbps. The PU considered here can be any MODEM or Wi-Fi enabled smart devices having the power consumption measurements as shown in Table 1 [40]. The SUs can be considered as devices like laptops, personal computers, tablets, etc. located anywhere in the campus. It has been assumed that the SUs in the proposed model can be present inside the various buildings across the campus at different distances from the FC as well as from the PU. Each SU participates individually to determine the vacant spectrum in CCSS. The SUs perform their local spectrum sensing and each of them provides a binary decision to the FC. As far as the fusion rules are concerned, a novel voting rule primarily motivated by the existing MAJORITY rule is used in this model as discussed in sub-section 2.2. The local sensing result indicates the presence/absence of any vacant spectrum and the decisions are fused at the FC.

TABLE 1 Power Consumption Measurements for Wi-Fi enabled devices [40,41]

Power Mode	Power Consumption
Active	Wi-Fi TX (+14dBm): 180mA Wi-Fi client: 130mA Wi-Fi Ap: 120mA Wi-Fi RX and listening: 97mA
Modem sleep	36mA (high speed: 240MHz) 30mA (at 160MHz) 24mA (normal speed: 80MHz)
Light sleep	0.8mA
Deep sleep	0.17mA (ULP co-processor is active) 0.12mA (ULP sensor-monitored pat- tern) 0.025mA (RTC timer + RTC memory)
Hibernate	5μA
Idle (no radios)	60mA

1.2 System model for DCSS

This model is developed following the Distributed Approach in CSS to address the problem of spectrum underutilization prevailing in rural areas as shown in Figure 3. As the Rural areas are underdeveloped having the scarcity of network towers, only limited spectrum is available for the network. Out of this available band, firstly it is needed to detect the vacant or un-used spectrum bands in order to facilitate communication effectively. In this model, the tower represents the PU; the white huts (H_{ij},i = 1, 2...n and j=1, 2...m) represent the SUs in a cluster having the cluster head (CH_i, i=

1, 2...n) marked as black coloured hut. Here, n and m denote the number of clusters and the number of SUs in each cluster respectively.

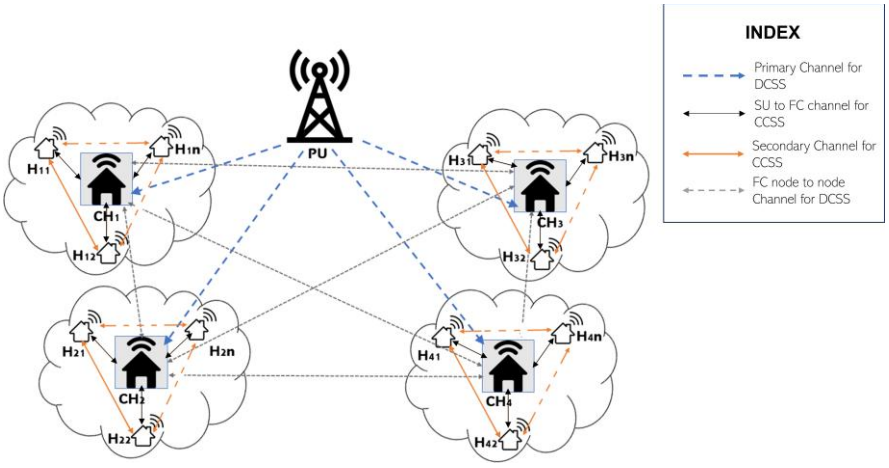

FIGURE 3 Proposed Model for Hybrid Distributed CSS in rural areas

The method of detecting the presence of PUs in the spectrum has been proposed in Figure 4. In the beginning of the sensing process, the active PUs and SUs need to be detected first. Then, all the hut clusters (1, 2, .., m) are scanned for the potential availability of free channels. For each of the individual clusters, sensing is done for the 1st to the *n*th nodes following the MAJORITY voting rule of CCSS. Given the low availability of spectrum in Rural areas, this rule provides the best performance for selecting vacant channels. After each cluster sends its decision to the local FC, the decision is compared against a particular value of detection potential (λ) and then selected by the distributed channel for efficient communication via the FC. This entire process is repeated $m \times n$ times until all the channels are exhausted and the process comes to a halt until the next sensing session starts.

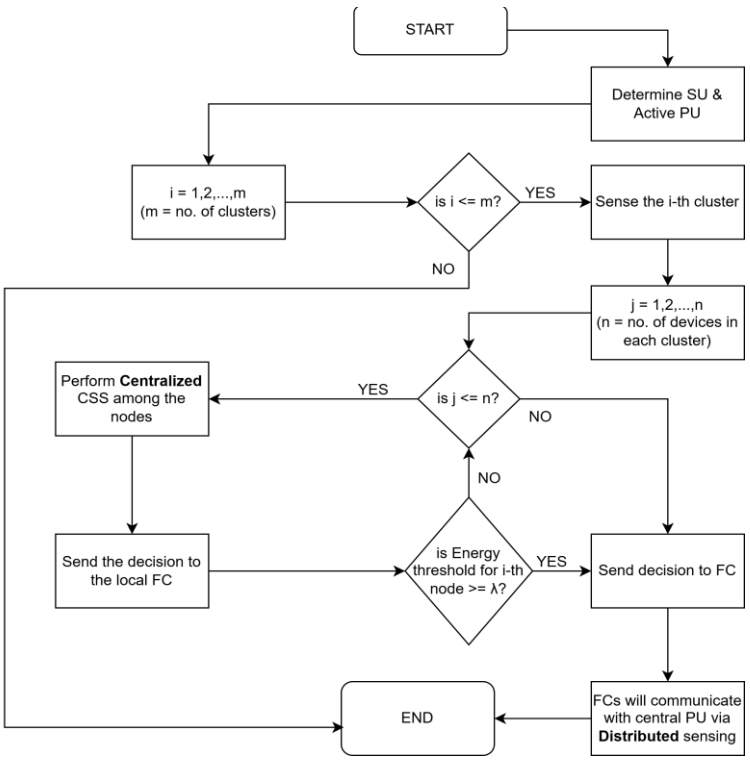

FIGURE 4 Flow chart for Energy Detection Technique in rural areas

A hybrid DCSS technique is adopted here for obvious reasons. For closely spaced huts in each zone of a rural communication system, CCSS is the best approach to detect the vacant spectrum. Generally, in Rural areas, the residential zones are bundled into distant clusters. In these cases, distributed sensing is the most effective method for inter-cluster data exchange. Therefore, a combination of both CSS methods is beneficial in this case.

In this approach, firstly, the local spectrum sensing is performed by each SU in a cluster. Subsequently, this information is exchanged between the other SUs (white huts) of the same cluster using the MAJORITY voting rule for its advantages as stated above to decide the presence of a PU. The information exchange between the SUs of the same cluster takes place considering Rayleigh fading environment as it is most suitable for indoor and small area outdoor non-line-of-sight communication. The decision made by the SUs based on the mutual probability of the presence of a PU is then sent to the Cluster Head (CH), the black huts in this case. Thus, each cluster has its final decision on the presence of a PU to its CH.

Since there are many such clusters present in the network, the various clusters are required to share the information between each other through their respective CHs using the derived voting fusion rule to finally decide on the presence of a PU. The CHs are mainly responsible for data reception, network management, and information sharing. The information sharing between the CHs is done using Weibull fading, which is well suited for multipath fading in outdoor environments over long-distance communication.

In this model, we have considered a range of approximately 20-30 km, which includes several villages. Moreover, each village is represented as a cluster consisting of multiple houses with an administrative house as the CH. Every common house, the SUs in this case, in a village communicates through the administrative house and eventually all the administrative houses from various clusters communicate with each other through the FC to establish a communication link among different villages. In this way, a decision will finally be made regarding the presence of the vacant band within this range.

1.3 System model for Combined Centralized and Distributed approach

The above models are combined together to propose a Combined Centralized and Distributed approach as shown in Figure 5 to establish the versatility of our proposed model for rural, suburban, and urban areas. The motivation is to provide a complete scenario of CSS for a practical Smart Network. Moreover, this model has been exposed to various real-life attenuation and fading conditions for long distance communication. This Combined Model has been grouped into Rural, Sub-Urban, and Urban zones based on the number of nodes per unit area, distance between the nodes, channel utilization pattern, physical structures and the presence of clutters in the path of communication which caters to fading and the severity of environmental conditions the channels might be exposed to. Based on these, the zone where the number of nodes is minimum and clustered into small bundles with large inter-cluster distances has been labeled as Rural. Here, the clutters present in the path of communication are mainly natural objects and the effect of fading due to rain and fog can be distinctly observed. The channel utilization pattern in this zone is sporadic. The zone where the number of nodes is intermediate between Rural and Urban node distribution and the nodal distances are lesser than the rural area, has been termed as Sub-Urban area. Here, the clutters in the path of communication are both man-made physical structures and natural objects.

The environmental attenuations are less prominent than the rural areas. Moreover, the channel utilization pattern in these zones varies with the time of the day. Finally, the zone with densely populated nodes, arbitrary channel utilization pattern with always heavy traffic load, large number of physical man-made barriers in the path of communication and lesser environmental attenuation impacts, has been identified as Urban zone. Here, the entire zone is a single large dense cluster with closely spaced devices. It is evident from the above description of the zones that environmental and other popular fading techniques will perform differently in each zone. Each zone of our proposed model is subjected to the available fading techniques along with environmental attenuations to test the converging nature of each model as well as their versatility.

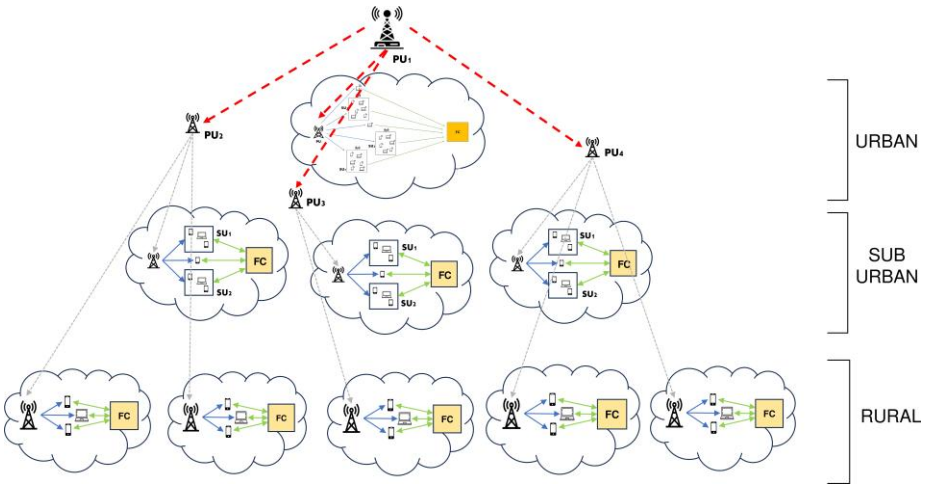

FIGURE 5 Proposed Model for Combined Centralized and Distributed CSS for Urban, Suburban and Rural Areas.

III. PERFORMANCE ANLAYSIS

The mathematical analysis of this work has been divided into four parts, namely energy detection technique, centralized spectrum sensing scheme, distributed spectrum sensing scheme, and the combined scheme. Energy detection scheme being the common aspect in all the subsequent sensing techniques, it has been formulated in the first sub-section.

3.1 Energy Detection Technique

The Energy detection (ED) technique is described in Figure 6 [4], where it receives the signal as

$$Y(t) = g.s(t)+n(t) \tag{1}$$

Where, $s(t)$ is the primary signal, g is the channel gain and $n(t)$ is the AWGN.

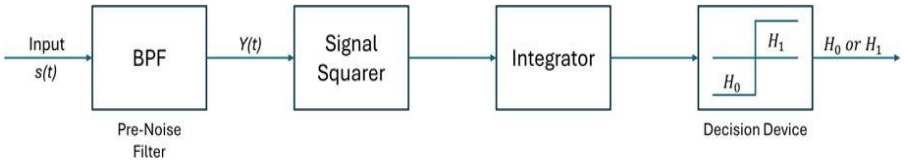

FIGURE 6 Block diagram for the energy detection technique.

It follows two hypotheses as listed below [1],[2]:

$$P = \begin{cases} n(t), & H_0 \\ g.s(t)+n(t), & H_1 \end{cases} \tag{2}$$

Here, H_0 and H_1 implies the presence and absence of a PU respectively.

The Probability of Missed Detection (P_m) and the Probability of False Alarm (P_f) are given by Eqs. (3) and (4) respectively [1, 2].

$$P_m = P\left(y(t) < \lambda / H_1 \right) = 1 - Q_{\tau w}(\sqrt{2\gamma}, \sqrt{\lambda}) \tag{3}$$

$$P_f = P\left(y(t) > \lambda / H_0 \right) = \frac{\Gamma(\tau_\omega, \frac{\lambda}{2})}{\Gamma(\alpha\omega)} \tag{4}$$

Where, λ is the threshold, τ_ω is the detection time, ω is the bandwidth, and γ is the SNR. The Detection Probability (P_d) [1, 2] is given by Eq. (5):

$$P_d = 1 - P_m = 1 - (1 - Q_{\tau\omega}(\sqrt{2\gamma}, \sqrt{\lambda})) = Q_{\tau\omega}(\sqrt{2\gamma}, \sqrt{\lambda}) \tag{5}$$

The Total Error (T.E.) function is obtained by combining P_f and P_m as depicted below:

$$T.E. = P_f + P_m = E(k, \lambda) \tag{6}$$

Where, k is the number of selected SUs from a set of M number of SUs. The Total Error Rate (TER) is easily calculated following Eq. (6) and subsequently used in the result section.

3.2 Centralized approach

For this approach, out of M SUs available for cooperation, we need to choose K SUs which will provide proper detection of vacant channels [8]. Here, our motivation has been to improve the channel utilization pattern without hampering the signal quality or increasing the sensing time. In other words, the objective has been to ensure the maximum channel utilization and the maximum channel throughput by proposing a new voting rule, which can give us the optimal number of SUs under the constraints of channel throughput, along with channel gain and sensing time. As the existing Majority Voting Rule [8] fails to perform under the aforementioned constraints, a novel voting rule has been proposed as follows:

Here, the T.E. obtained from Eq. (6) is minimized to obtain an optimized value of K (K_{opt}), keeping throughput, channel gain, and sensing time as constraints. Thus, minimizing (K, λ), we obtain

$$\frac{\partial E(K, \lambda)}{\partial K} \geq 0 \approx E(K+1, \lambda) - E(K, \lambda) \geq 0 \tag{7}$$

Using the partial differential formula, we get

$$\frac{\delta}{\delta x} s(x, y) = s(x \pm 1, y) - s(x, y) \tag{8}$$

Which gives,

$$[P(H_1)P_m(K \pm 1, \lambda) + P(H_0)P_f(K \pm 1, \lambda)] - [P(H_1)P_m(K, \lambda) + P(H_0)P_f(K, \lambda)] \geq 0 \tag{9}$$

Now,

$$P_m = 1 - \sum_{j=K_{\text{opt}}}^{M} \binom{M}{j} (1 - P_m)^j \, P_m^{M-j} \tag{10}$$

$$P_f = \sum_{j=K_{\text{opt}}}^{M} \binom{M}{j} (1 - P_f)^{M-j} \, P_f^j \tag{11}$$

Therefore,

$$\begin{aligned} &- \sum_{j=K_{\text{opt}}+1}^{M} (1 - P_m)^j P_m^{M-j} + \sum_{j=K_{\text{opt}}+1}^{M} (1 - P_f)^{M-j} P_f^j \\ &\geq - \sum_{j=K_{\text{opt}}}^{M} (1 - P_m)^j P_m^{M-j} + \sum_{j=K_{\text{opt}}}^{M} (1 - P_f)^{M-j} P_f^j \end{aligned} \tag{12}$$

Simplifying the above equation and taking the summand function, we get,

$$-\binom{M}{K_{\text{opt}+1}}\left(1-P_m\right)^{K_{\text{opt}+1}} P_m^{M-K_{\text{opt}+1}} + \binom{M}{K_{\text{opt}+1}}\left(1-P_f\right)^{M-K_{\text{opt}+1}} P_f^{K_{\text{opt}+1}} \geq$$
$$-\binom{M}{K_{\text{opt}}}\left(1-P_m\right)^{K_{\text{opt}}} P_m^{M-K_{\text{opt}}} + \binom{M}{K_{\text{opt}}}\left(1-P_f\right)^{M-K_{\text{opt}}} P_f^{K_{\text{opt}}} \tag{13}$$

$$\Rightarrow (1-P_m)^{K_{opt}} P_m^{M-K_{opt}} \times \left[1-(K_{opt}+1)(M-K_{opt}+1)(1-P_m)P_m\right] \geq$$
$$(1-P_f)^{M-K_{opt}} P_f^{K_{opt}} \times \left[1-(K_{opt}+1)(M-K_{opt}+1)(1-P_f)P_f\right] \tag{14}$$

Ignoring the small value terms, we get,

$$\Rightarrow \left(1-P_m\right)^{K_{\text{opt}}} P_m^{M-K_{\text{opt}}} \geq \left(1-P_f\right)^{M-K_{\text{opt}}} P_f^{K_{\text{opt}}} \tag{15}$$

$$\Rightarrow K_{\text{opt}}\left\{\ln(1-P_m)-\ln P_f\right\} + K_{\text{opt}}\left\{\ln\left(1-P_f\right)-\ln P_m\right\} \geq M * \ln\left(1-P_f\right) \tag{16}$$

Which can be further modified into Eq. 17 and 18 as shown below:

$$K_{\text{opt}} \geq \frac{M\ln(1-P_f)}{\ln(1-P_m)+\ln(1-P_f)-(\ln P_f+\ln P_m)} \tag{17}$$

$$\Rightarrow K_{\text{opt}} \geq \frac{M\ln(1-P_f)}{\ln(1-P_m)(1-P_f)-(\ln P_f P_m)} \tag{18}$$

The above mathematical formulation describes the new voting rule named as Max Throughput Voting Rule (MTVR) which has been proposed here for obtaining the optimal number of SUs.

3.3 *Distributed approach*

In this approach, the nodes within each cluster communicate following the MAJORITY voting rule as given by Eq. (19) [8] in a Rayleigh fading environment [8, 17].

$$\textit{Majority Rule} \rightarrow \begin{cases} P_{m,t} = 1 - \sum_{j=\frac{N}{2}}^{N} \binom{N}{j} (1-P_m)^j P_m^{N-j} \\ P_{f,t} = \sum_{j=\frac{N}{2}}^{N} \binom{N}{j} (1-P_f)^{N-j} P_f^j \end{cases} \tag{19}$$

The Pd in Rayleigh fading environment is described as

$$\overline{P_{d\text{Ray}}} = e^{-\frac{\lambda}{2}} \sum_{k=0}^{m-2} \frac{1}{k!}\left(\frac{\lambda}{2}\right)^k + \left(\frac{1+\bar{\gamma}}{\bar{\gamma}}\right)^{m-1}\left[e^{-\frac{\lambda}{2(1+\bar{\gamma})}} - e^{-\frac{\lambda}{2}} \sum_{k=0}^{m-2} \frac{1}{k!}\left(\frac{\lambda\bar{\gamma}}{2(1+\bar{\gamma})}\right)^k\right] \tag{20}$$

The central hut from each cluster acts as a FC and all such FCs communicate with each other in a distributed sensing manner using the MTVR as stated in Eq. (18) improvised for a Weibull fading environment for a long-range multipath fading communication. The P_d in Weibull fading environment is given by

$$\overline{P_{d_{\text{wei}}}} = \sum_{l=0}^{u-1} \frac{\lambda^l e^{-\lambda/2}}{l!\,2^l} + \sum_{l=0}^{\infty} \frac{(-1)^l A^l \lambda^u}{l!\,u!\,2^u \bar{\gamma}^{lu/2} e^{\lambda/2}} \Gamma\left(\frac{la}{2}+1\right) {}_1F_1\left(\frac{la}{2}+1, u+1, \frac{\lambda}{2}\right) \tag{21}$$

Where, $A = \left[\Gamma\left(1+\frac{2}{a}\right)\right]^{a/2}$. The expression ${}_1F_1(a,b,z)$ denotes Kummer's confluent hypergeometric function, which is defined as ${}_1F_1(a,b,z) = \sum_{n=0}^{\infty} \frac{(a)_n z^n}{(b)_n n!}$ where, $(a)_n = \frac{\Gamma(a+n)}{\Gamma(a)}$ is known as the Pochhammer symbol [7].

It may be mentioned here that in general, distributed CSS follows AND-AND, AND-OR, OR-AND or OR-OR voting rules, but in our case, we have used the Majority-MTVR rule which theoretically decreases T.E. and thus increases the overall throughput of the system.

3.4 *Combined approach*

For the combined approach, the zones are divided as shown in Figure 5. Each zone has been tested for their respective fading models as given by the Eqs. (18), (20), and (21). Along with these, atmospheric attenuations due to rain and fog have been considered as they are greatly dependent on the diverse range of each zone. Rain attenuation is a major challenge to satellite communication, especially at frequencies above 10 GHz. The most popular rain prediction model, the ITU-R model [30], is a statistical model based upon a factor derived from R (rain rate in mm/hr), link frequency (1-1000 GHz) and curve fitting parameters K_{rain} and α which are functions of polarization elevation angle and polarization tilt angle.

In this work, the above rain attenuation model has been modified for CSS over the frequency band of 1-3.5 GHz, which is considered as the range of working frequency. After obtaining the specific attenuation A (dB/km), we have estimated the attenuation of radio waves due to rain over a longer distance path. Here, specific attenuation in dB/km is given by

$$A(K_{\text{rain}}, R) = K_{\text{rain}} R^{\alpha} \tag{22}$$

Where K_{rain} is defined as:

$$K_{\text{rain}} = \frac{K_H + K_V + (K_H - K_V)\cos^2\theta\cos(2\tau)}{2} \tag{23}$$

and,

$$\alpha = \frac{K_H\alpha_H + K_V\alpha_V + (K_H\alpha_H - K_V\alpha_v)\cos^2\theta\cos(2\tau)}{2}$$

Where, K_H and α_H are horizontal local polarization parameters, K_V and α_V are vertical local polarization parameters. θ is the link elevation angle and τ is the polarization tilt angle.

Now, introducing a new distance parameter d in the formula, which signifies the range of communication network, we get the cumulative attenuation along the entire path length d, given by

$$A_{\text{total}} = A(K_{\text{rain}}, R) \cdot d \tag{24}$$

Moreover, to assess the impact of rain attenuation on CSS, the impact of the received signal power (P_r) at the receiver has also been considered as stated in Eq. (25).

$$P_r(f, R, d) = P_t \times 10^{-\frac{A_{\text{total}}(f, R, d)}{10}} \tag{25}$$

Where, f is a constant which depends on the specific frequency of operation. Considering above modifications in the rain attenuation model, the SNR at the receiver end (S_r) is calculated as:

$$S_r = \frac{P_r}{N_0} \tag{26}$$

Where, N_0 is the noise signal.

Substituting the value of γ with S_r in Eq. (3) and applying it to Eq. (18), we get the modified value of K_{opt} for CSS considering rain attenuation model as shown in Eq. (27)

$$K_{opt} \geq \frac{M \cdot \ln\left(1 - \frac{\Gamma(\tau_\omega, \lambda/2)}{\Gamma(\tau_\omega)}\right)}{\ln\left(Q_{\tau_\omega}\left(\sqrt{2S_r}, \sqrt{\lambda}\right) \cdot \frac{\Gamma(\tau_\omega, \lambda/2)}{\Gamma(\tau_\omega)}\right) - \ln\left(\frac{\Gamma(\tau_\omega, \lambda/2)}{\Gamma(\tau_\omega)} \cdot \left(1 - Q_{\tau_\omega}\left(\sqrt{2S_r}, \sqrt{\lambda}\right)\right)\right)} \tag{27}$$

Where λ is given by,

$$\lambda = \sqrt{2N_0\sigma^2}\, Q^{-1}(P_f) + N_0\sigma^2\omega \tag{28}$$

Here, σ^2 is the noise variance.

Taking into consideration the impact of fog, the SNR due to fog attenuation γ_{fog} is given by Eq. (29):

$$\gamma_{fog} = K_l(f) \times M \tag{29}$$

Here, $K_l(f)$ represents the specific attenuation coefficient based on frequency, and M denotes the liquid water density in g/m^3.

Therefore, the modified value of K_{opt} for CSS considering fog attenuation model can be obtained by substituting S_r in Eq. (27) by γ_{fog} giving Eq. (30):

$$K_{opt} \geq \frac{M \cdot \ln\left(1 - \frac{\Gamma(\tau_\omega, \lambda/2)}{\Gamma(\tau_\omega)}\right)}{\ln\left(Q_{\tau_\omega}\left(\sqrt{2\gamma_{fog}}, \sqrt{\lambda}\right) \cdot \frac{\Gamma(\tau_\omega, \lambda/2)}{\Gamma(\tau_\omega)}\right) - \ln\left(\frac{\Gamma(\tau_\omega, \lambda/2)}{\Gamma(\tau_\omega)} \cdot \left(1 - Q_{\tau_\omega}\left(\sqrt{2\gamma_{fog}}, \sqrt{\lambda}\right)\right)\right)} \tag{30}$$

IV. RESULTS AND DISCUSSIONS

This section highlights the performance analyses of the pro- posed models as well as their comparative analyses with some of the relevant existing works. MATLAB R2023b has been used as the simulation tool for this work. This section has been divided into three sub-sections: Firstly, sub-section 4.1 analyses the performance of the CCSS based Urban Model with respect to ROC curves and TER function; Secondly, in sub- section 4.2, DCSS based Rural Model has been simulated incorporating the proposed hybrid voting rules as required for two stage distributed sensing and compared its performance with other contrast models, which uses existing voting rules. The results have been analyzed with respect to ROC curves. Lastly, in sub-section 4.3 we have incorporated different types of environmental fading factors to simulate the combined model. The specific attenuation due to rain and fog has been calculated and compared with different models proposed in this work, namely, Rural, Sub-Urban and Urban with respect to varied distances and frequencies. The performance of the developed model is also compared with other existing works.

4.1 Performance analysis of CCSS based Urban Model

4.1.1 Simulation scenario and parameters for CCSS based Urban Model

We have considered a densely populated city with many mobile users and closely spaced mobile towers. The simulation parameters are set according to the IEEE 802.16 Metropolitan Area Network [39] standard which is listed in the Table 2. IEEE 802.16 has been used because this is a well-established standard for broadband wireless access, ensuring stability and compatibility. Choosing this standard also lays the groundwork for advancing spectrum sensing as well as wireless network efficiency and investigating newer standards (e.g., IEEE 802.11ax, 5G NR) for comparative analysis [39]. The model has been tested under all kind of fading channel conditions available at an urban level namely, AWGN, Rayleigh, Nakagami and Rician.

Table 2 IEEE 802.16 MAN [39]

Parameters	**Values**
Range	1-10km
Data Rate	1-70Mbps
Spectrum	2.5-3.5GHz
Bandwidth	1.25-28MHz
User Carriers	200
Pilot Carriers	8
Modulation	BPSK QPSK 16-QAM 64-QAM

For the simulation in Figure 8, the values of different parameters are taken from table 4:

Table 4 Parameter list for ROC simulations of different fading scenarios.

Parameters	**Value**
Omega (ω)	1
PU	1
SU	5 (calculated optimum)
No. of ROCs	1000
SNR (dB)	0-10

4.1.2 *Simulation results for CCSS based Urban Model*

Figure 7 depicts the effect of SNR (dB) on probability of error for both simulationand analytical scenarios considering three types of fading, namely Nakagami, Rayleigh and Rician.

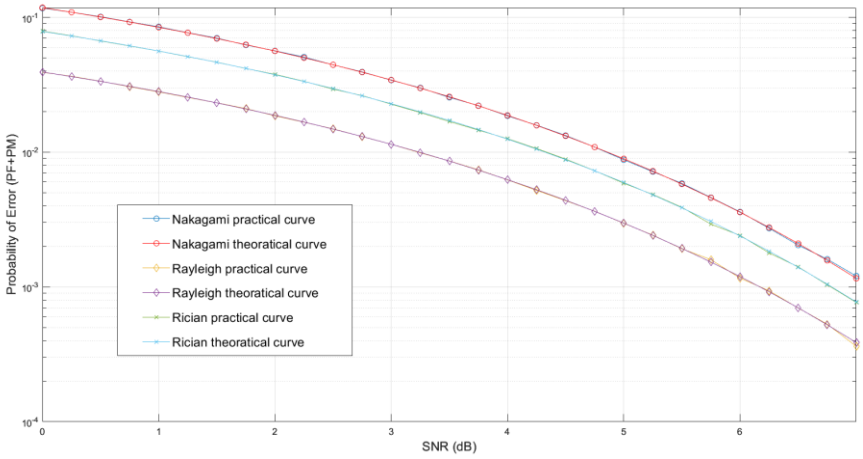

Fig. 7 Probability of Error versus Signal to Noise Ratio

It is clearly visible that Probability of Error decreases with the increasing valueof SNR, as good signal strength implies lesser possibility of missed detection. More- over, Nakagami and Rayleigh fading offers the highest and lowest probability of errorrespectively; whereas, Rician fading based curves lie in between. These facts are justified as follows: The indoor-Rayleigh fading is mainly used for indoor non line of sightcommunication thus providing the lowest probability of error; whereas, Nakagami fading is meant for outdoor and metropolitan communication environment thus leadingto the highest probability of error. As Rician fading is considered for both indoor and outdoor communication environments considering the clutters in the path of communication, it offers moderate probability of error in between the aforementioned cases. It has also been observed that proposed model is marginally stable as the simulated curves approach to the analytical curves very closely under three different fading scenarios. The detailed analysis in this regard has been presented in Table 3.

Table 3 Comparison table of Error Probability for different fading channels

FadingChanel	**SNR(dB)**	**Probability of Error (Analytical)**	**Probability of Error (Simulated)**
Rayleigh	2.50	0.01487	0.01488
	4.50	0.00439	0.00436
	5.75	0.00156	0.0016
	6.75	0.00052	0.00053
Rician	2.50	0.029	0.0293
	4.50	0.0087	0.0088
	5.75	0.0030	0.0029
	6.75	0.00104	0.000103
Nakagami	2.50	0.0445	0.0445
	4.50	0.0131	0.0132
	5.75	0.0045	0.0046
	6.75	0.0015	0.0016

Figure 8 shows the ROC curves for the CCSS based Urban model subjected to different fading scenarios.

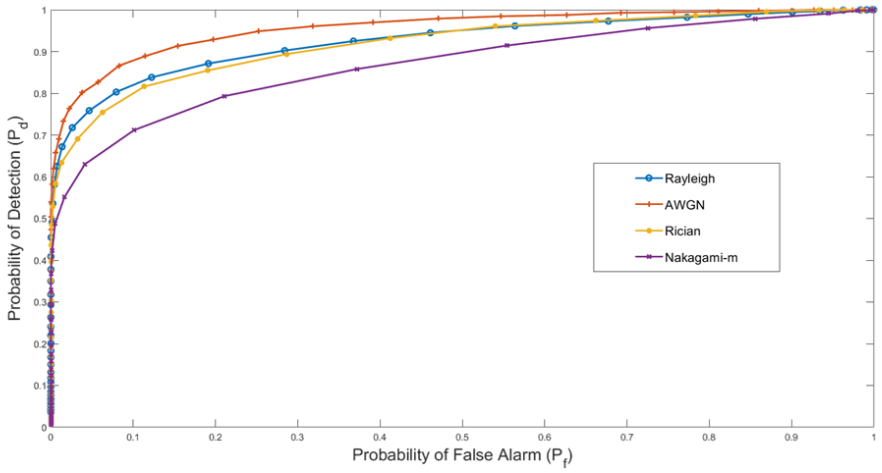

Fig. 8 ROC curves for the centralized CSS based urban model subjected to different fading scenarios

It is evident that the AWGN channel offers the highest value of P_d with a lower value of P_f among other channel models. As far as Rayleigh and Rician channel conditions are considered, Rayleigh fading gives better P_d value compared to Rician fading at lower values of P_f. For higher values of P_f, they almost coincide with each other. This is for the reason that Rayleigh is suitable for more general non-LOS communication compared to Rician, which is considered for both indoor and outdoor communication environments considering the clutters in the path of communication. Nakagami-m gives the lowest value of P_d compared to others as it is used for more flexible modelling with or without LOS path. It can be mentioned that when the valueof Nakagami factor (m) equal to 0.5, Nakagami distribution approaches to Gaussian distribution; for $m = 1$, Nakagami distribution becomes Rayleigh distribution; and for $m > 1$, Nakagami distribution approaches Rician distribution [42].

Finally, figure 9 shows the plot of TE versus Threshold for different voting rules.

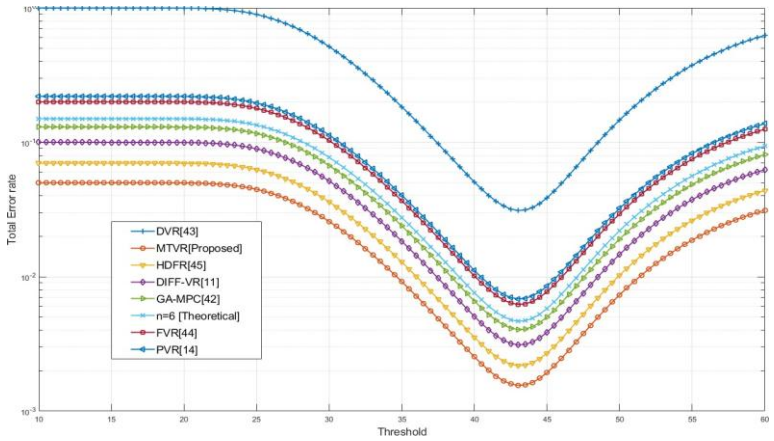

Fig. 9 Comparison curves for various voting rules

Here, Six voting rules namely, Default Voting Rule (DVR) [43], Proposed Voting Rule (PVR) [14], Fading Voting Rule (FVR) [44], Hard Decision Fusion Rule (HDFR)[45], Differential Voting Rule (Diff-VR) [11] and Statistical Genetic Algorithm basedvoting rule (GA-MPC) [42] have been compared with the proposed Max Throughput Voting Rule (MTVR). It can be clearly stated that the proposed MTVR outperforms other existing voting rules.

Table 5 Comparison of TE of different voting rules atSNR 5 dB and n=6

Voting Rule	Threshold	Total Error (TE)
DVR [43]	43	0.031
PVR [14]	43	0.007
FVR [44]	43	0.006
GA-MPC [42]	43	0.004
Diff-VR [11]	43	0.003
HDFR [45]	43	0.002
MTVR (proposed)	43	0.001

Table 5 gives a comparative analysis of our developed voting rule (MTVR) with other existing ones. It is evident that the proposed MTVR offers the least value ofTE amongst other voting rules.

4.2 Performance analysis of DCSS based Rural Model

4.2.1 Simulation scenario and parameters for DCSS based Rural Model

For a rural model, we have selected a regional area where the huts are arranged intosparsely spaced clusters. Each cluster can communicate with the other. The numberof towers is less and spaced at large distances. The simulation parameters for inter and intra cluster communication are set according to the IEEE 802.22 Wireless Regional Area Network (WRAN) [39] and IEEE 802.11 WLAN [39] standard as shown in Table 6 and 7 respectively. The model has been tested for different fusion voting rulesapplicable to a distributed network.

Table 6 IEEE 802.22 WRAN Parameters [39]

Parameters	Values
Range	17 - 30 km
Data Rate	1 - 10 Mbps
Spectrum	54 - 862 MHz
Max. no. of CPEs (CustomerPremise Equipments)	512
Modulation	For 15 km, 64-QAM For 22 km, 16-QAM For 30 km, QPSK

Table 7 IEEE 802.11 WLAN Parameters [39]

Parameters	Values
Operating frequency range	470 - 510 MHz
Channel bandwidth	6 MHz
Transmission Power	20 dBm
Modulation format	BPSK
Antenna Gain	0, 1, 2 dBi

4.2.2 Simulation results for DCSS based Rural Model

The graph below represents the study of P_d versus SNR using different fusion rulesfor DCSS model.

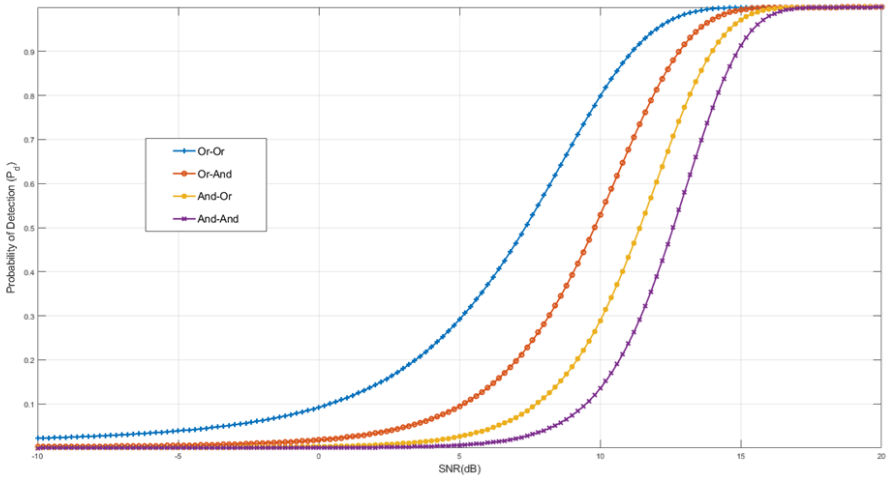

Fig. 10 Probability of Detection (P_d) versus SNR curve for different fusion voting rules for D-CSS

From the above graph we can see that as the SNR value increases, the P_d value alsoincreases for all the fusion rules. It is evident that any OR based fusion rule exhibits better performance in terms of P_d than any AND based rule following the logical OR and AND operations. Accordingly, OR-OR and AND-AND fusion rule provides the maximum and minimum value of P_d respectively. Moreover, the P_d curves for OR- AND and AND-OR fusion rules lie in between the above curves, where, OR-AND rule outperforms the AND-OR rule for the obvious reason. Since any OR based rule offers a higher value of P_f and any AND based rule provides a higher value of P_m, soa trade-off has been made to choose the appropriate fusion rule to be applied in our proposed DCSS model. The negative SNR value has been incorporated to show the detection ability of the OR rule even under the presence of a very weak signal.

The comparative analysis is summarized in Table 8 which justifies the above discussion.

Table 8 Detection Probability (P_d) for different Fusion Rules

Fusion-Rule	**SNR (dB)**	**P_d**
OR-OR	5	0.2918
OR-AND		0.0947
AND-OR		0.0261
AND-AND		0.0064
OR-OR	10	0.7984
OR-AND		0.5287
AND-OR		0.2889
AND-AND		0.1351
OR-OR	15	0.9995
OR-AND		0.9943
AND-OR		0.9716
AND-AND		0.9129

In Figure 11, we have compared our proposed hybrid distributed CSS model withother CSS based distributed models considering different fading and types of networks.

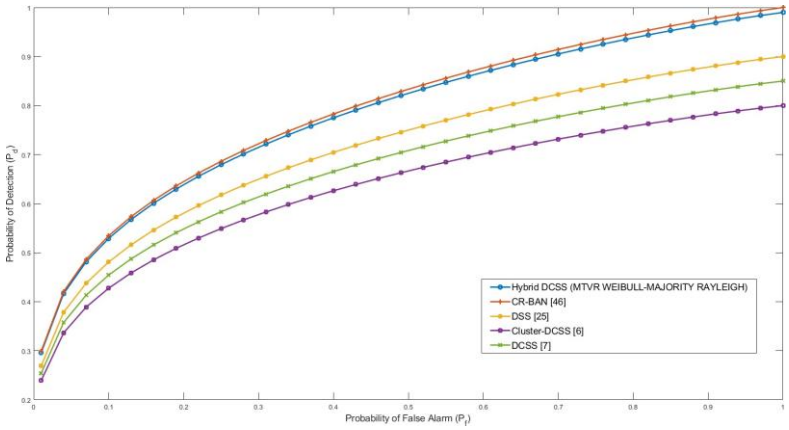

Fig. 11 P_d versus P_f curves for different D-CSS models

It is seen that in all cases, with the increasing value of P_f, P_d also increases. The curve which finally bends more towards unity, shows better outcomes. As evident from the above figure, our hybrid model outperforms the existing models [6], [7], [25] other than [46] which uses CR-BAN. The model in [46] provides better probability of detection than the proposed model and other DCSS models because CR-BAN is restricted to a cluster of smart wearable devices and smart household gadgets within a building. So, the fading environment is considered as indoor Rayleigh fading which is less severe compared to other decentralized models. Moreover, the higher cluster node density in CR-BAN provides higher detection accuracy compared to other distributed sensing models. However, our proposed model has its own advantages. The proposed Hybrid DCSS model is more useful for rural regions, where the clusters are sparsely spaced as well as the number of devices per cluster is less and the fading environment is dynamic. This architecture extends network coverage to remote areas when some of the cluster fails under emergency conditions. The model also dynamically adjusts to interference fluctuations present in the rural regions. This communication network enables effective agricultural monitoring, smart farming and other rural communication needs as well.

4.3 Performance analysis of the Proposed Combined Model

The proposed model is a combination of the Rural and Urban models leading to a suburban setup as described in 3.4. This model is subjected to various atmospheric attenuation factors such as rainfall and fog as described in the subsequent sub-sections.

4.3.1 Analysis under the presence of rain attenuation

4.3.1.1 Simulation scenario and parameters for rain attenuation model

For signal attenuation due to rainfall, we have used Eqs. (24) and (27). We have taken the distance range between 1 to 10 km and spectrum range of up to 3.5 GHz. The weather data for this set of simulations was recorded on 30/06/2023 fromAccuWeather website [50] by selecting Kolkata (22.5744°N, 88.3629°E) as the Urban zone, Sunderbans (21.9497°N, 89.1833°E) as the Rural zone and Diamond Harbour (22.1927°N, 88.1895°E) as the Sub-Urban zone. These data are summarized in Table 9.

Table 9 Parameter list for rain attenuation model [34]

Parameters	**Urban**	**Rural**	**Semi-Urban**
Range (km)	1-10	17-30	30-100
Frequency (GHz)	2.5-3.5	2.5-3.5	2.5-3.5
Light rain (mm/hr)	0.5-2	0.5-2	0.5-2
Moderate rain (mm/hr)	2-4	2-4	2-4
Heavy rain (mm/hr)	4-8	4-8	4-8
Very heavy rain (mm/hr)	>8	>8	>8

4.3.1.2 Simulation results for rain attenuation model

The figure below depicts the rain attenuation of the RF signal ranging from 1 to3 GHz for our Sub-Urban model, subjected to different distances.

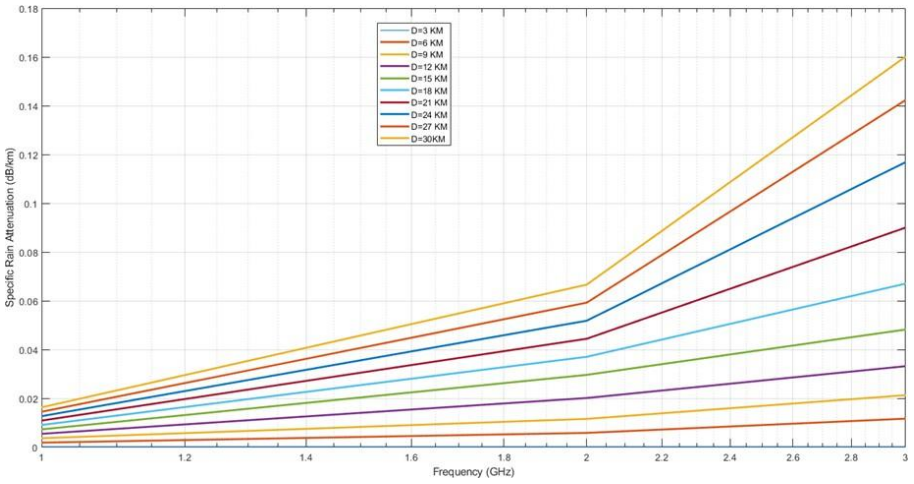

Fig. 12 Variation of Rain Attenuation with frequency for different distances

Here, we can see that with increase in the range of network, the signal attenuationdue to rainfall also increases according to Eq. 24. It is also found that up to a frequency of 2 GHz, a gentler slope is observed indicating gradual increase in signal attenuation, after which, the presence of steeper slope implies an increase in signal loss which becomes higher at higher frequencies and higher distances. Figure 13 shows the effectof the range of network on the specific rain attenuation when the Frequency is variedfrom 1 GHz to 3.5 GHz.

Fig. 13 Variation of specific rain attenuation with distance for different frequencies

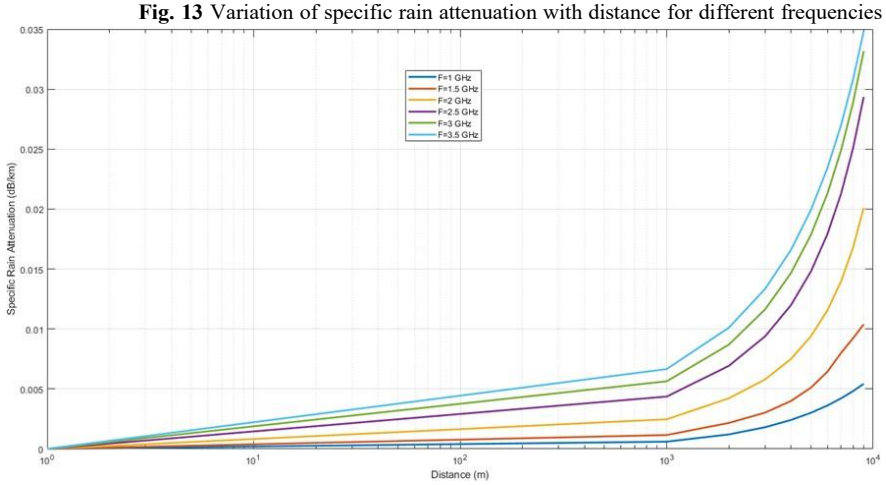

Here also, we find linear increase in signal attenuation with increase in frequencyup to a distance of 1km, after which, the signal attenuation increases exponentially with a very steep slope, indicating the rapid attenuation of signals between a distanceof 1 and 10 km. Figure 14 gives an interesting study of the effects of type of rainfall over signal attenuation within the working frequency range of 2.5 to 3.5 GHz.

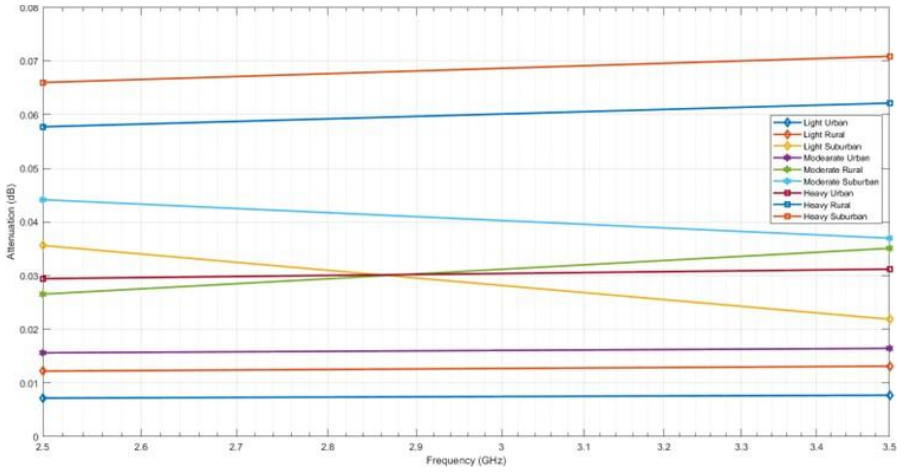

Fig. 14 Variation of rain attenuation with frequency for different rain rates at different regions

In general, signal attenuation increases with increased amount of rainfall, where light and heavy rainfall having the minimum and maximum effect on signal attenuation respectively, for each of the individual regions; whereas, the effect of moderaterainfall on signal attenuation falls in-between. Region-wise analysis is summarized as follows: Firstly, for Urban region, it is found that for light and moderate rainfall, signal attenuation almost remains constant within the working range of frequency from 2.5 GHz to 3.5 GHz. However, for heavy rainfall, slight linear increase in signal attenuation is observed over the given range of frequency as expected theoretically [30]. Secondly, for Rural region, the signal attenuation is almost independent of frequencyfor light rainfall; whereas, both heavy and moderate rainfall exhibits an increased effect of signal attenuation with frequency due to the increased effect of wet foliage [27]. Lastly, for Sub-Urban region, for moderate and light rainfall, the signal attenuation decreases with frequency due to lesser effect of wet foliage than rural region andsparsely placed mobile towers than urban region. Attenuation in this region is mainlydominated by geophysical observations such as rain structure, raindrop size distribution, wind direction, etc. [27]. However, for heavy rainfall, the signal attenuation is mainly dominated by type of rainfall rather than the region wise network behavior, thus signal attenuation increases linearly with frequency, as expected [27]. Figure 15gives the comparison of our developed model with other two statistical models, threeoptimization models, two empirical models and two physical models for rain attenuation. For this purpose, the working range of frequency of our proposed work has been extended to 10^3 GHz to accommodate the aforementioned models. Moreover, the rainfall rate for this simulation has been taken as the average value of the high, low and moderate rainfall.

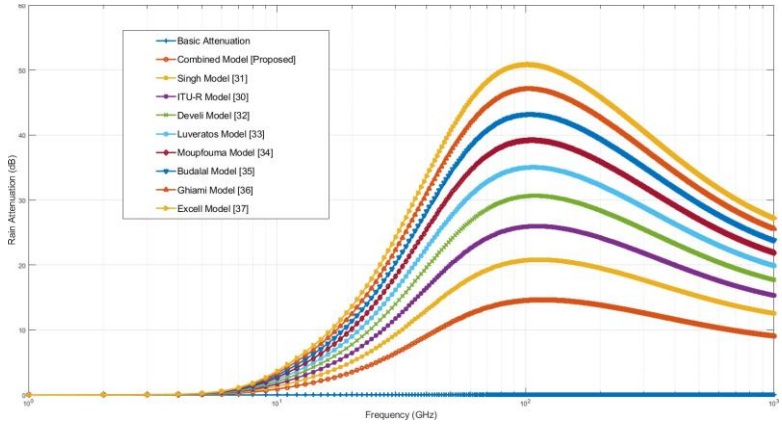

Fig. 15 Comparison curves with other Rain attenuation models

The findings have been enlisted in Table 10 for three different values of frequencysuch as, 3.5 GHz, 10^1 GHz and 10^2 GHz. The rain attenuation (dB) correspondingto the frequency values of 3.5 GHz and 10^1 GHz have been observed by zooming the curves in live editor of MATLAB 2023(b). From the values of attenuation, we can

clearly say that our rain prediction model offers the minimum attenuation compared to other rain attenuation models over the frequency range of 1-10^3GHz. Moreover, whenthe attenuation values are compared with those of Figure 14, it has been observed that both resemble over the frequency range 2.5 GHz to 3.5 GHz.

Table 10 Rain attenuation model comparisons

AttenuationModel	Attenuation (dB) for 3.5GHz	Attenuation (dB) for 10^1 GHz	Attenuation (dB) for 10^2 GHz	Performance Improvement in Attenuation (%) at 10^2 GHz
Combined (Pro-posed)	0.018	0.90	14.54	0.00
Singh [31]	0.020	1.32	20.71	29.79
ITU-R [30]	0.030	1.69	25.90	43.86
Develi [32]	0.040	2.03	30.57	52.44
Luveratos [33]	0.043	2.36	34.98	58.43
Moupfouma [34]	0.050	2.69	39.15	62.86
Budalal [35]	0.066	3.01	43.17	66.32
Ghiami [36]	0.074	3.34	47.00	69.06
Excell [37]	0.082	3.66	50.83	71.39

4.3.2 Analysis under the presence of fog attenuation

4.3.2.1 Simulation scenario and parameters for fog attenuation model

To analyze the effect of fog on signal attenuation Eq. (30) has been used. Forthis purpose, the proposed combined model has been subjected to various distances and frequencies for Rural, Urban and Sub-Urban regions. The relevant data for this set of simulations was recorded on 30/12/2023 at 6 a.m. from AccuWeather website [50] with Kolkata (22.5744°N, 88.3629°E) as the selected Urban zone, Sunder- bans (21.9497°N, 89.1833°E) as the selected Rural zone and Diamond Harbour (22.1927°N, 88.1895°E) as the selected Sub-Urban zone. This is depicted in Table 11.

Table 11 List of parameters for fog attenuation [38]

Parameters	Urban	Rural	Sub-Urban
Distance (km)	1-10	17-30	30-100
Frequency (GHz)	2.5-3.5	2.5-3.5	2.5-3.5
Humidity (%)	52	60	65
Temperature (°C)	20	15	18
Pressure (Pa)	101600	100815	100610
LWD (g/m^3)	0.15	0.4	0.25

4.3.2.2 Simulation results for fog attenuation model

Figure 16 gives the variation of the fog attenuation with frequencies for differentdistances.

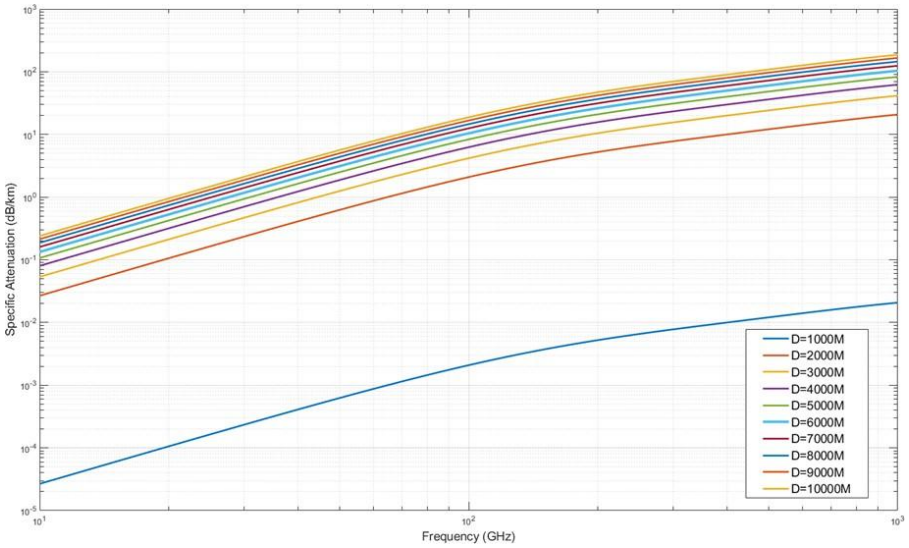

Fig. 16 Variation of specific attenuation due to fog with frequency for different distances

We find that with the increase in distance; attenuation also increases with the increase in frequency. It is also observed that up to a distance of 1 km, the attenuationis much lower, after which it increases abruptly. For example, the attenuation levels for a distance of 2 km, 3 km and 4 km are 0.027 dB/km, 0.053 dB/km and 0.08 dB/km respectively, at a frequency of 10^1 GHz. As the distance is further increased,a little increase in attenuation level is observed for a particular frequency. Figure17 presents the variation of specific attenuation due to fog with distances over the working frequency range of 2.5 to 3.5 GHz.

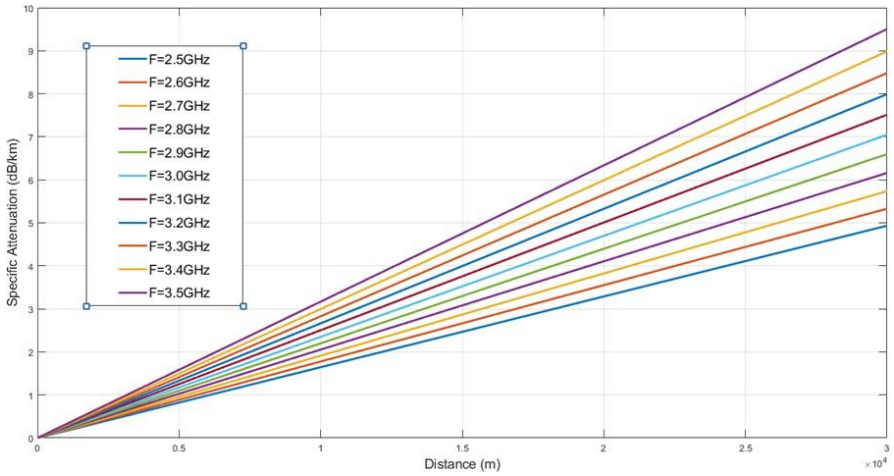

Fig. 17 Variation of fog attenuation with distance over the working frequency range (2.5-3.5GHz)

It is evident that fog attenuation graphs are closely spaced linear curves up to adistance of 5 km, beyond which, the spacing between the lines starts increasing.

Figure 18 below gives the specific attenuation due to fog for Urban, Sub-Urban andRural regions within our working range of frequency (2.5 to 3.5 GHz).

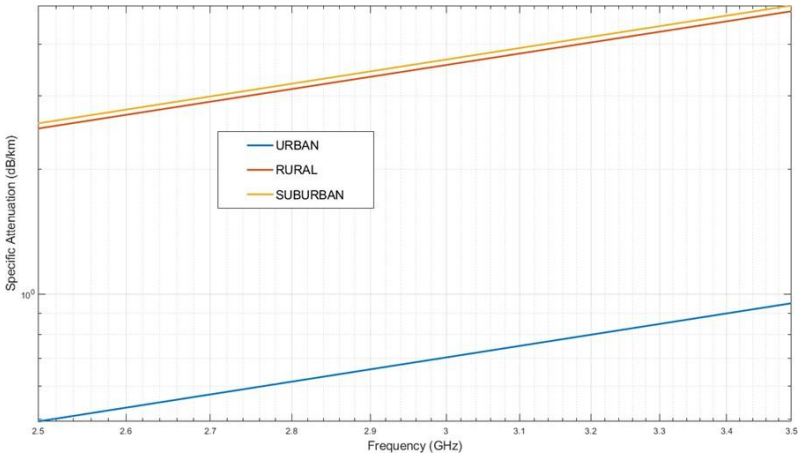

Fig. 18 Specific attenuation due to fog for various regions

From Figure 18 above, we can clearly say that specific attenuation due to fog ismore visible for Rural and Sub-Urban areas compared to urban areas.

Figure 19 below gives a comparative analysis of different fog attenuation models withour proposed model, all scaled down to a frequency range of 0-10 GHz.

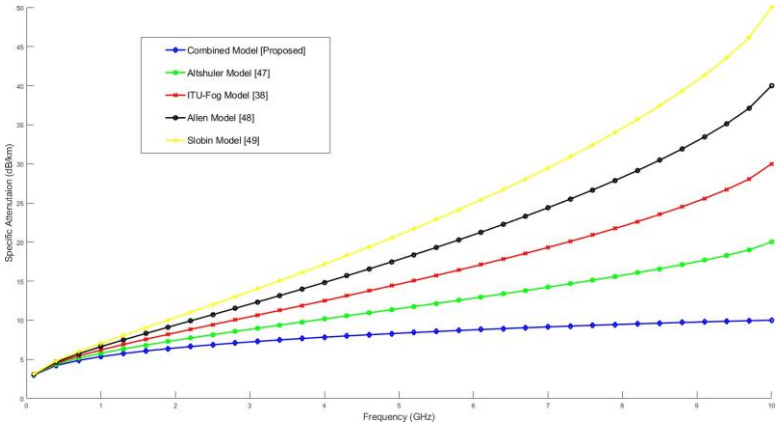

Fig. 19 Comparison curves for different fog attenuation models

The analysis is summarized in Table 12. It is evident that our proposed model gives minimum specific attenuation for our selected distance and communication frequency range.

Table 12 Specific Attenuation (dB/km) at Various Frequencies

Model	**2 GHz**	**3 GHz**	**4 GHz**	**6 GHz**	**10 GHz**
Combined Model (proposed)	6.3	7.3	7.8	8.8	10.0
Altshuler Model [47]	7.2	8.9	10.1	13.0	20.0
ITU-Fog [38]	8.0	10.6	12.5	17.1	30.0
Allen Model [48]	9.0	12.3	14.8	21.3	40.0
Slobin Model [49]	10.0	14.0	17.2	25.4	50.0

4.4 Overall Performance Analysis

Figure 20 gives an overall comparative analysis of the Combined Model interms of P_d and P_f . Here, we have considered a test case of our proposed Urban CCSS model subjected to different fading scenarios namely, Rayleigh, Rician, Nakagami and AWGN. Our proposed combined model has also been subjected to rain and fog attenuation for the urban network range.

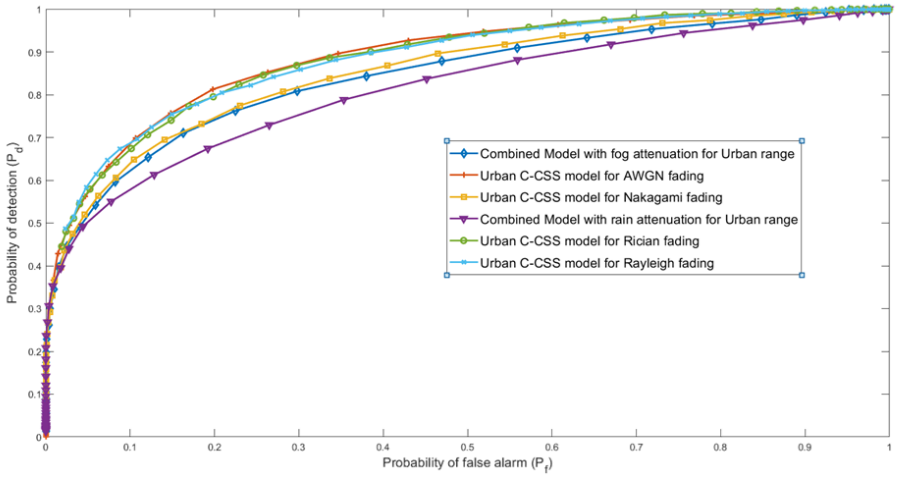

Fig. 20 ROC curves for various attenuation models of CSS

Here we find that, AWGN channel gives the best and the Combined Model with rain attenuation gives the least value of P_d for any specific value of P_f. Moreover, the curves for Combined Model with fog attenuation almost coincides with the Urban-CSS model for Nakagami Fading, thus establishing the fact that the Combined Model behaves as a CSS based Urban Model when the range is limited to Urban network.

The overall comparison of the proposed models with some of the existing models have also been analyzed in terms of resource consumption and overall system cost have been depicted in Figure 21 and 22 respectively. Here, the resource consumption has been analyzed mainly in terms of Energy Consumption and Bandwidth Utilization considering IEEE 802.16, 802.11 and 802.22 standards [51] as shown in Figure 21. The overall system cost is calculated in terms of Infrastructure Cost, Installation Cost, Maintenance Cost, Upgradation Cost and Software Cost [52]. While calculating the Infrastructure Cost, no Base Station related cost is included as we have assumed that the existing Base Stations have been utilized in all models. So, costs related to APs, Wireless Controllers, Switches, Hubs and Routers, Wireless Network Interface Cards, Antennas and Cables, etc. have been mainly considered under the Infrastructure Cost [53]. The analysis of the Overall System Cost has been depicted in Figure 22.

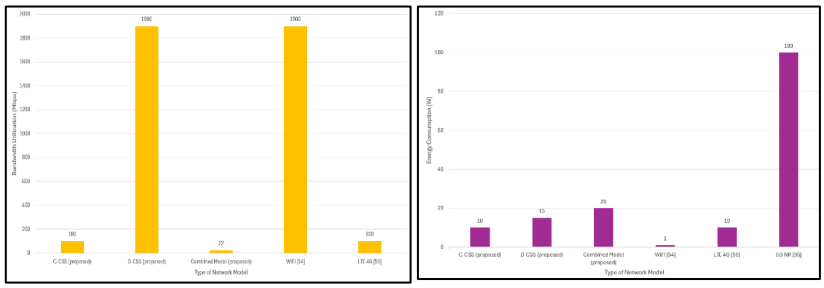

a. Bandwidth Utilization b. Energy Consumption

Fig. 21 Overall Resource Consumption analysis

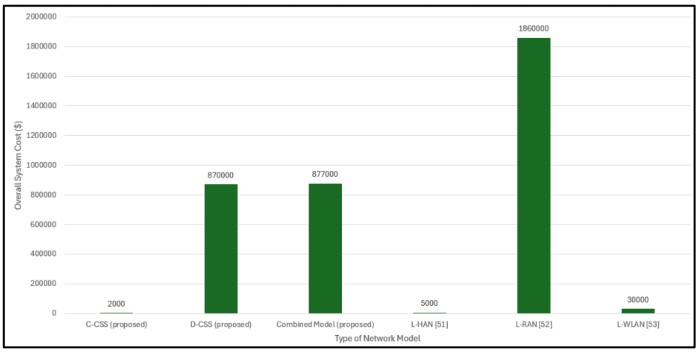

Fig. 22 Overall System Cost analysis

Finally, the Scalability of the proposed models has been discussed with the increased number of SUs or nodes. This is to note that all the proposed models presented in this paper are based on three different IEEE standards, namely, IEEE 802.11, IEEE 802.16 and IEEE 802.22. More precisely, the first proposed model or C-CSS model primarily focuses on urban environment. So, it is based on IEEE 801.16 (WiMax) standard. Accordingly, it can support up to 1000 subscribers per sector theoretically [51]. Since the second proposed or D-CSS model primarily targets the rural environment, it follows IEEE 802.11 (WLAN) standard which can support up to 100 nodes per AP for intracell communication theoretically [53]. The third proposed or Combined model is meant for all three environments such as, rural, urban and suburban. So, following the IEEE 802.22 (WRAN) standard, it can support 1000 users per cell for intercell communications theoretically [39]. Following this discussion, we can say that all our proposed models are highly scalable where the proposed Combined model and C-CSS model offers the highest and lowest degree of scalability respectively, placing the proposed D-CSS model in between.

It is noteworthy that although our proposed models are capable to provide high scalability, it cannot achieve the theoretical targets due to several challenges posed by the networks such as increased complexity, network congestion, Quality of Service (QoS) degradation, network instability, security issues etc. apart from resource constraints [54].

V. CONCLUSION

CSS based CR networks ranging from rural, sub-urban and urban have been coveredin this paper. The networks have been subjected to different kind of fading conditions as well as atmospheric attenuations. In the first part, a MAN has been implemented and a new voting rule based on Centralized CSS has been developed. When it is tested against the existing rules, it is found to outperform them under the proposed conditions. In the second part, a CSS based RAN has been developed. Hybrid voting rules have been applied on this to study the performance of the RAN, which provides better probability of detection compared to the other related sensing models for DCSS. In the final part of the paper, we have proposed a combined model for Sub-Urban networks. This model has been subjected to various kind of atmospheric attenuationfactors such as rain and fog. It is found that the proposed model outperforms the existing rain and fog attenuation models when frequency range is scaled down to theoperating range of the proposed work. Finally, an overall comparison on the performance of the combined model with the CCSS based Urban model has been analyzed considering all fading conditions. As an extension to this work, the versatility of the proposed models could be tested for other ranges of terrestrial communication. This work could be further extended by incorporating the effect of atmospheric gases intoour model so that it could be beneficial for Industrial IoT applications. Another good scope of future work could be addressing the major challenges posed by the mobile CR users in a distributed sensing environment namely, Dynamic Topology, Intermittent Connectivity, Location-Dependent Spectrum Availability, Handover Latency, etc. Accordingly, our proposed combined model could be modified to accommodate the above factors to make it more dynamic, versatile and realistic.

Data Availability

No datasets were generated or analyzed during the current study.

Competing interests

The authors have no financial or non-financial interest to disclose.

Funding

No funding was received to assist with the preparation of this manuscript.

Authors' contributions

All the authors have taken part in the research work, problem statement formulation, simulation of results, preparing the manuscript and rechecking of the paper.

.

ACKNOWLEDGMENT

We are grateful to the Department of ETCE, Jadavpur university for providing us with the laboratory facilities to carry out this research. We are also thankful to the Department of CST, CSIT, CSE-Networks, CSE-Cybersecurity from the Institute of Engineering and Management Kolkata, University of Engineering and Management Kolkata for providing us their IEDC Laboratory facilities to work constantly on this paper and improve the research findings.

REFERENCES

[1] Nasser, A., Al Haj Hassan, H., Abou Chaaya, J., Mansour, A., Yao, K.-C.: Spectrum sensing for cognitive radio: Recent advances and future challenge. Sensors 35 21(7), 2408 (2021)

[2] Ganesan, G., Li, Y.: Cooperative spectrum sensing in cognitive radio, part ii: multiuser networks. IEEE Transactions on wireless communications 6(6), 2214 2222 (2007)

[3] Letaief, K.B., Zhang, W.: Cooperative communications for cognitive radio networks. Proceedings of the IEEE 97(5), 878–893 (2009)

[4] Digham, F.F., Alouini, M.-S., Simon, M.K.: On the energy detection of unknown signals over fading channels. In: IEEE International Conference on Communica tions, 2003. ICC'03., vol. 5, pp. 3575–3579 (2003). IEEE

[5] Anjana, S., Nandan, S.: Energy-efficient cooperative spectrum sensing: A review. In: 2018 Second International Conference on Inventive Communication and Computational Technologies (ICICCT), pp. 992–996 (2018). IEEE

[6] Sharma, G., Sharma, R.: Performance comparison of centralised and distributed css over fading channels in cognitive radio. Cogent Engineering 4(1), 1355599 (2017)

[7] Sharma, Y., Sharma, R., Sharma, K., Sharma, G.: Cooperative spectrum sensing over weibull and hoyt fading channels using centralized and distributed schemes. In: 2020 3rd International Conference on Emerging Technologies in Computer Engineering: Machine Learning and Internet of Things (ICETCE), pp. 197–201 (2020). IEEE

[8] Shinde, S.C., Jadhav, A.N.: Performance comparison of centralized cooperative spectrum sensing based on voting rules in cognitive radio. International Journal of Advanced Engineering Research and Science 3(5), 236722 (2016)

[9] Bouraoui, R., Besbes, H.: Cooperative spectrum sensing for cognitive radio networks: Fusion rules performance analysis. In: 2016 International Wireless Communications and Mobile Computing Conference (IWCMC), pp. 493–498 (2016). IEEE

[10] Sun, H., Nallanathan, A., Jiang, J., Wang, C.-X.: Cooperative spectrum sens ing with diversity reception in cognitive radios. In: 2011 6th International ICST Conference on Communications and Networking in China (CHINACOM), pp. 216–220 (2011). IEEE

[11] Nallagonda, S., Bhowmick, A., Prasad, B.: Throughput performance of cooper ative spectrum sensing network with improved energy detectors and sc diversity over fading channels. Wireless Networks 27(6), 4039–4050 (2021)

[12] Rauniyar, A., Jang, J.M., Shin, S.Y.: Optimal hard decision fusion rule for centralized and decentralized cooperative spectrum sensing in cognitive radio 36 networks. Journal of Advances in Computer Networks 3(3), 207–212 (2015)

[13] Bhowmick, A., Nallagonda, S., Roy, S.D., Kundu, S.: Cooperative spectrum sens ing with double threshold and censoring in rayleigh faded cognitive radio network. Wireless Personal Communications 84, 251–271 (2015).

[14] Banavathu, N.R., Khan, M.Z.A.: Joint optimization of both m and k for the m out-of-k rule for cooperative spectrum sensing. In: European Wireless 2018; 24th European Wireless Conference, pp. 1–6 (2018). VDE

[15] Althunibat, S., Di Renzo, M., Granelli, F.: Optimizing the k-out-of-n rule for cooperative spectrum sensing in cognitive radio networks. In: 2013 IEEE Global Communications Conference (GLOBECOM), pp. 1607–1611 (2013). IEEE

[16] Banavathu, N.R., Khan, M.Z.A.: Optimization of n-out-of-k rule for heteroge neous cognitive radio networks. IEEE Signal Processing Letters 26(3), 445–449 (2019)

[17] Ghosh, S.K., Trankatwar, S.R., Bachan, P.: Optimal voting rule and minimization of total error rate in cooperative spectrum sensing for cognitive radio networks. Journal of Telecommunications and Information Technology (2021)

[18] Singh, A., Bhatnagar, M.R., Mallik, R.K.: Cooperative spectrum sensing in mul tiple antenna based cognitive radio network using an improved energy detector. IEEE Communications letters 16(1), 64–67 (2011)

[19] Nallagonda, S., Chandra, A., Roy, S.D., Kundu, S.: Performance of improved energy detector based cooperative spectrum sensing over hoyt and rician faded channels. IEICE Communications Express 2(7), 319–324 (2013)

[20] Ranjeeth, M., Behera, S., Nallagonda, S., Anuradha, S.: Optimization of coopera tive spectrum sensing based on improved energy detector with selection diversity in awgn and rayleigh fading. In: 2016 International Conference on Electrical, Electronics, and Optimization Techniques (ICEEOT), pp. 2402–2406 (2016). IEEE

[21] Verma, P.K., Soni, S.K., Jain, P.: Performance evolution of ed-based spectrum sensing in cr over nakagami-m/shadowed fading channel with mrc reception. AEU-International Journal of Electronics and Communications 83, 512–518 (2018)

[22] Huang, H., Yuan, C.: Cooperative spectrum sensing over generalized fading channels based on energy detection. China Communications 15(5), 128–137 (2018)

[23] Ben Halima, N., Boujemaa, H.: Cooperative spectrum sensing with dis tributed/centralized relay selection. Wireless Personal Communications 115(1), 37 611–632 (2020)

[24] Ben Halima, N., Boujemaa, H.: Cooperative spectrum sensing with dis tributed/centralized relay selection. Wireless Personal Communications 115(1), 611–632 (2020)

[25] Mokhtar, R.A., Saeed, R.A., Alhumyani, H.: Cooperative fusion architecture based distributed spectrum sensing under rayleigh fading channel. Wireless Personal Communications 124(1), 839–865 (2022)

[26] Kesavan, U., Islam, M.R., Abdullah, K., Tharek, A.: Rain attenuation predic tion for higher frequencies in microwave communication using frequency scaling technique. In: 2014 International Conference on Computer and Communication Engineering, pp. 217–219 (2014). IEEE

[27] Isabona, J., Imoize, A.L., Rawat, P., Jamal, S.S., Pant, B., Ojo, S., Hinga, S.K.: Realistic prognostic modeling of specific attenuation due to rain at microwave frequency for tropical climate region. Wireless Communications and Mobile Computing 2022(1), 8209256 (2022)

[28] Li, L., Sali, A., Wali, S.Q.: Attenuation of mmwave based on measured data via rain sensor in tropical region. In: 2022 IEEE 6th International Symposium on Telecommunication Technologies (ISTT), pp. 50–55 (2022). IEEE

[29] Rubavathy, A., Sundar, S.: A review of cooperative approach for mitigation of fading. In: AIP Conference Proceedings, vol. 2966 (2024). AIP Publishing

[30] Regonesi, E., Luini, L., Riva, C.: Limitations of the itu-r p. 838-3 model for rain specific attenuation. In: 2019 13th European Conference on Antennas and Propagation (EuCAP), pp. 1–4 (2019). IEEE

[31] Singh, H., Kumar, V., Saxena, K., Boncho, B., Prasad, R.: Proposed model for radio wave attenuation due to rain (rwar). Wireless Personal Communications 115, 791–807 (2020)

[32] Develi, I.: Differential evolution based prediction of rain attenuation over a los terrestrial link situated in the southern united kingdom. Radio Science 42(03), 1–6 (2007) https://doi.org/10.1029/2006RS003615

[33] Livieratos, S.N., Cottis, P.G.: Rain attenuation along terrestrial millimeter wave links: A new prediction method based on supervised machine learning. IEEE Access 7, 138745–138756 (2019) https://doi.org/10.1109/ACCESS.2019.2939498

[34] Samad, M.A., Diba, F.D., Choi, D.-Y.: A survey of rain attenuation predic tion models for terrestrial links—current research challenges and state-of-the-art. Sensors 21(4), 1207 (2021) 38

[35] Budalal, A.A.H., Islam, M.R., Abdullah, K., Rahman, T.A.: Modification of dis tance factor in rain attenuation prediction for short-range millimeter-wave links. IEEE Antennas and Wireless Propagation Letters 19(6), 1027–1031 (2020)

[36] Ghiani, R., Luini, L., Fanti, A.: A physically based rain attenuation model for terrestrial links. Radio Science 52(8), 972–980 (2017)

[37] Capsoni, C., Fedi, F., Paraboni, A.: A comprehensive meteorologically oriented methodology for the prediction of wave propagation parameters in telecommuni cation applications beyond 10 ghz. Radio Science 22(3), 387–393 (1987)

[38] Singh, H., Kumar, V., Saxena, K., Prasad, R.: A smart model for prediction of radio wave attenuation due to clouds and fog (smrwacf). Wireless Personal Communications, 1–19 (2022)

[39] Cordeiro, C., Challapali, K., Birru, D., Shankar, S.: Ieee 802.22: the first world wide wireless standard based on cognitive radios. In: First IEEE International Symposium on New Frontiers in Dynamic Spectrum Access Networks, 2005. DySPAN 2005., pp. 328–337 (2005). Ieee

[40] Khan, A.A., Rehmani, M.H., Reisslein, M.: Cognitive radio for smart grids: Sur vey of architectures, spectrum sensing mechanisms, and networking protocols. IEEE Communications Surveys & Tutorials 18(1), 860–898 (2015)

[41] Y¨ uksel, M.E.: Power consumption analysis of a wi-fi-based iot device. Electrica 20(1), 62–71 (2020)

[42] Godugu, K.K., Vappangi, S.: Performance evaluation of hard-decision and soft data aided cooperative spectrum sensing over nakagami-m fading channel. IET Communications 17(13), 1492–1512 (2023)

[43] Zhang, W., Mallik, R., Letaief, K.: Optimization of cooperative spectrum sensing with energy detection in cognitive radio networks. IEEE Transactions on Wireless Communications 8, 5761–5766 (2009) https://doi.org/10.1109/TWC.2009.12.081710

[44] Majumdar, S., Chattopadhyay, S., Ghatak, S.R., Biswas, V.: Throughput and error function joint optimization for css based field area network under vari ous fading environments. In: 2020 IEEE Applied Signal Processing Conference (ASPCON), pp. 330–334 (2020). IEEE

[45] Liu, X., Zheng, K., Chi, K., Zhu, Y.: Cooperative spectrum sensing optimization in energy-harvesting cognitive radio networks. IEEE Transactions on Wireless Communications PP, 1–1 (2020) https://doi.org/10.1109/TWC.2020.3015260

[46] Alqahtani, A.S., Changalasetty, S.B., Parthasarathy, P., Thota, L.S., Mubarakali, A.: Effective spectrum sensing using cognitive radios in 5g and wireless body 39 area networks. Computers and Electrical Engineering 105, 108493 (2023) https: //doi.org/10.1016/j.compeleceng.2022.108493

[47] https://www.accuweather.com/

[48] Altshuler, E.E., Marr, R.A.: Cloud attenuation at millimeter wavelengths. IEEE Transactions on antennas and propagation 37(11), 1473–1479 (1989)

[49] Liebe, H.J., Allen, K.C., Hand, G.R., Espeland, R., Violette, E.: Millimeter-wave propagation in moist air: Model versus path data. NTIA Report, 85–171 (1985)

[50] Slobin, S.D.: Microwave noise temperature and attenuation of clouds: Statistics of these effects at various sites in the united states, alaska, and hawaii. Radio Science 17(6), 1443–1454 (1982)

[51] Molla, T.: Smart home energy management system. In Research Anthology on Smart Grid and Microgrid Development (2022)

[52] Popescu, V., Fadda, M., Murroni, M.: Performance analysis of ieee 802.22 wire less regional area network in the presence of digital video broadcasting–second generation terrestrial broadcasting services. IET Communications 10 (2016)

[53] Chochul, M., ˇ Sevˇc´ ık, P.: A survey of low power wide area network technologies. In: 2020 18th International Conference on Emerging eLearning Technologies and Applications (ICETA), pp. 69–73 (2020). https://doi.org/10.1109/ICETA51985.2020.9379213

[54] Pramono, S., Alvionita, L., Ariyanto, M.D., Sulistyo, M.E.: Opti mization of 4G LTE (long term evolution) network coverage area in sub urban. AIP Conference Proceedings 2217(1), 030193 (2020) https://doi.org/10.1063/5.0000732 https://pubs.aip.org/aip/acp/article pdf/doi/10.1063/5.0000732/14053909/030193 1 online.pdf

[55] Rinaldi, F., Raschell`a, A., Pizzi, S.: 5g nr system design: a concise survey of key features and capabilities. Wireless Networks 27(8), 5173–5188 (2021) https: //doi.org/10.1007/s11276-021-02811-y

[56] Morais, D.H.: Wi-fi 6 overview. Springer Nature Switzerland, 131–156 (2023)